Available online at www.sciencedirect.com
ScienceDirect
Sensors and Actuators B 125 (2007) 301–310
SENSORS AND ACTUATORS B CHEMICAL
www.elsevier.com/locate/snb

Neural network and Bayesian network fusion models to fuse electronic nose and surface acoustic wave sensor data for apple defect detection

Changying Li [a,*], Paul Heinemann [b], Richard Sherry [c]

[a] Department of Agricultural and Biological Engineering, University of Illinois at Urbana-Champaign, 376C AESB, MC-644, 1304 W. Pennsylvania Avenue, Urbana, IL 61801, United States
[b] Department of Agricultural and Biological Engineering, The Pennsylvania State University, University Park, United States
[c] School of Information Sciences and Technology, The Pennsylvania State University, University Park, United States

Received 26 October 2006; received in revised form 9 February 2007; accepted 10 February 2007
Available online 20 February 2007

Abstract

The Cyranose 320 electronic nose (Enose) and zNose™ are two instruments used to detect volatile profiles. In this research, feature level and decision level multisensor data fusion models, combined with covariance matrix adaptation evolutionary strategy (CMAES), were developed to fuse the Enose and zNose data to improve detection and classification performance for damaged apples compared with using the individual instruments alone. Principal component analysis (PCA) was used for feature extraction and probabilistic neural networks (PNN) were developed as the classifier. Three feature-based fusion schemes were compared. Dynamic selective fusion achieved an average 1.8% and a best 0% classification error rate in a total of 30 independent runs. The static selective fusion approach resulted in a 6.1% classification error rate, which was not as good as using individual sensors (4.2% for the Enose and 2.6% for the zNose) if only selected features were applied. Simply adding the Enose and zNose features without selection (non-selective fusion) worsened the classification performance with a 32.5% classification error rate. This indicated that the feature selection using the CMAES is an indispensable process in multisensor data fusion, especially if multiple sources of sensors contain much irrelevant or redundant information. At the decision level, Bayesian network fusion achieved better performance than two individual sensors, with 11% error rate versus 13% error rate for the Enose and 20% error rate for the zNose. It is shown that both the feature level fusion with the CMAES optimization algorithms and decision level fusion using a Bayesian network as a classifier improved system classification performance. This methodology can also be applied to other sensor fusion applications.

Keywords: Multisensor data fusion; Electronic nose; zNose; Apple; Evolutionary strategy; Bayesian network; Artificial neural networks; Probabilistic neural networks; Back-propagation network

1. Introduction

Apples (*Malus domestica*, Borkh) are one of the most frequently consumed fruits in the United States and the world at large. The United States is the second largest apple producing country with nearly 5 million tonnes total production and 1.7 billion dollars in revenue (2004) [1]. Pennsylvania is the fifth largest U.S. apple producing state, accounting for roughly 4% of the national production [2].

Apples are usually stored for as much as 6–10 months before arriving at grocery stores and being sold to customers. During this long storage period, spoilage and diseases may occur. The most common apple postharvest diseases are *Botrytis cinerea* Pers., *Penicillium expansum* Link, *Mucor piriformis* [3]. It is estimated that typically more than 10% of harvested apples are lost due to spoilage [4]. Controlled atmosphere (CA) technology has been widely adopted for apple storage by reducing the temperature, and adjusting oxygen and carbon dioxide levels to inhibit the metabolic activities of apples. Under this confined storage condition, it is impossible for humans to enter the storage room and visually inspect apple conditions. Hence, any spoilage and diseases go undetected, resulting in economic losses. At the retail level, store managers want to assure that each bag of apples contains only good quality individuals, devoid of spoilage and disease. However, some spoiled apples are occluded by healthy apples within a plastic bag and may not be detected visually.

* Corresponding author. Tel.: +1 217 244 3925; fax: +1 217 244 0323.
E-mail address: cyli@uiuc.edu (C. Li).

0925-4005/$ – see front matter © 2007 Elsevier B.V. All rights reserved.
doi:10.1016/j.snb.2007.02.027

From the perspective of both storage managers and retailers, there is a need to develop a non-invasive, sensitive, and fast method to detect apple spoilage.

Prior studies have shown that compositional changes in volatiles occur during fruit ripening, and vary depending on the presence of diseases and physical damage [5]. By detecting these changes, deteriorated apples can be detected and differentiated from healthy apples. The electronic nose, developed in 1982 [6], has been widely used in food quality control, medical diagnosis, and homeland security [7–9]. Several research groups have applied the Enose to predict fruit (apple, pear, and banana) ripeness [10–12]. It has also been used for quality sorting of blueberries [5], spoilage identification of beef [13], peanut off-flavor detection [14], sausage fermentation monitoring [15], grain quality inspection [16] and for other food products [17,18]. Unlike analytical chemical instruments such as gas chromatography and mass spectrometry (GC–MS), the electronic nose does not detect and identify single volatiles, but differentiates smell patterns of vapor mixtures by using pattern recognition algorithms. Its processing time for the electronic nose is also much faster than for GC–MS. This characteristic gives the Enose a distinct advantage over GC–MS in certain applications when concern is not about the specific volatile compounds, but the overall smell patterns, such as food quality inspection and class differentiation.

Multisensor data fusion techniques try to combine data from multiple sensors, with the objective of making better inferences (less uncertainty, lower error rate) regarding a physical entity, event, activity or situation than using individual sensors alone. To be successful, the additional sensors must provide complementary information [19]. Usually, more diverse sources of data provide more information and result in better performance. For instance, humans and animals use multiple senses to improve their chances of survival. They use not only their vision system, but hearing, smell, and taste to determine if a product is edible. Typically, selection of good sensors and proper fusion processing techniques are two key components of a successful multi-sensor data fusion problem. The data fusion process was first developed by the Department of Defense (DoD) and used for the location, characterization and identification of weapon systems and military units [20]. It has also been widely used in nonmilitary applications such as the implementation of robotics, medical diagnosis using multiple instruments, and environmental monitoring (e.g., locating earth quakes, characterizing hurricanes) [19]. Mathematical algorithms, which are used to implement data fusion, are drawn from traditional disciplines such as digital signal processing, statistics, control theory, and artificial intelligence. They include Kalman filtering, clustering analysis, artificial neural networks, Bayesian inference, Dempster-Shafer's method, etc. [21]. Several attempts have been made to apply multisensor data fusion methods to fuse data from different sensors and improve the performance of fruit quality inspection systems [22–26].

Two volatile sensing instruments, the Enose and zNose, were applied to detect apple spoilage in the research described in this paper. Both of these instruments have previously been used separately for food quality evaluation [27,28]. In this research, the data from these two instruments were combined to improve the classification performance using multisensor data fusion techniques.

Two different levels of data fusion models were explored. The data from the two commercial volatile sensing instruments were combined at the feature level and the decision level. In the feature level fusion, features were extracted from the Enose and zNose using principal component analysis (PCA) and these extracted features were fed into artificial neural networks (ANN) for classification. The optimization method covariance matrix adaptation evolutionary strategy (CMAES) was applied to select relevant sensors that provide complementary information and to optimize the fusion model. Three different feature-based fusion models were implemented and compared. In the decision level fusion, a Bayesian network was used to fuse classification results after these two instruments made a declaration of identity.

2. Methods

2.1. Data measurement

The Enose (Smith Detection, Herts, UK) consists of 32 internal thin film carbon black polymer composite sensors, which can function at ambient air temperature. The resistance from these conducting chemiresistors increases when vapor-phase analytes adsorb on the surface and disrupt the conductive pathways [29]. These 32 composite polymer sensors are non-specific to a wide range of volatile compounds and are capable of recognizing odors with a pattern recognition system. The zNose (Electronic Sensor Technology, Newbury Park, CA) consists of one capillary column and one surface acoustic wave (SAW) sensor. Volatile compounds that pass through the capillary column are separated based on their different solubility and enter the SAW sensor at different times. The oscillating frequency from the SAW sensor changes due to the mass change caused by volatile compound surface deposition and results in a frequency shift with respect to elution time. Examples of both the Enose and zNose signals are shown in Fig. 1.

Red 'Delicious' apples were purchased from a local grocery store and were intentionally damaged by inducing a 10 mm deep cross-slice cut on the top. These damaged apples were exposed to room air for deterioration development. The measurements were conducted every other day from day 4 to day 14 after the cut treatment. Other apples without the cut treatment were considered "healthy" apples. Apple samples were kept in room air for 6 h to reach the ambient air temperature before each test. The equilibrium time for headspace concentration was also 6 h. Apples were maintained at room air temperature (20 ± 1 °C) for 48 h between each measurement. A 2 L glass jar was used as a headspace gas concentration chamber, sealed by a plastic cap with a Teflon septum.

The Enose was used to sample volatile compounds emitted by the apples by inserting a 50 mm long snout needle into the 5 mm hole in the lid of the glass jar. These measurements were stored in the Enose and downloaded to the computer by an RS 232 cable. The zNose was equipped with a 5 cm long sampling needle at the inlet, which was inserted into the concentration

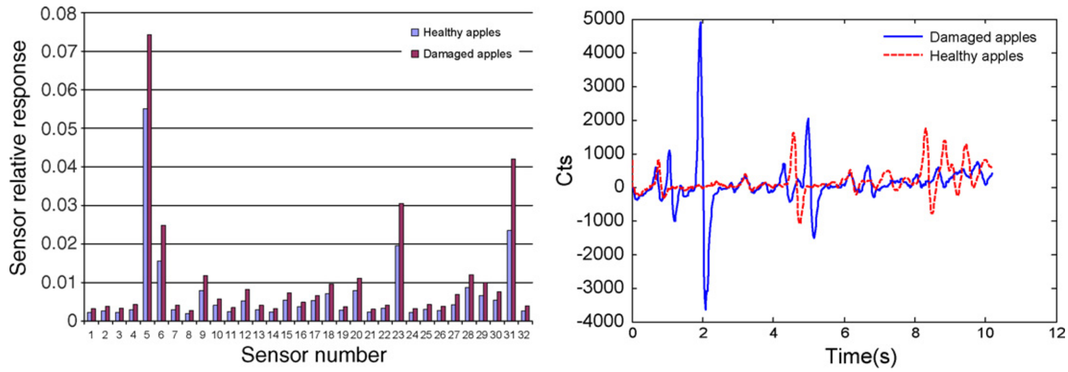

Fig. 1. Enose and zNose “smellprint” samples.

chamber for sampling. The sampling time was 10 s, during which the gas sample was released from the trap inside the system and carried over the column (DB-5) in a helium flow of 3 cm^3/min. The SAW sensor was heated to 125 °C for 5 s after each data sampling period to clean the SAW detector. One blank system purge run was conducted between each sample measurement to attain a stable baseline.

Sampling was conducted at three different times: March, June, and September, 2005. The sampling time and number of samples for each group are shown in Table 1.

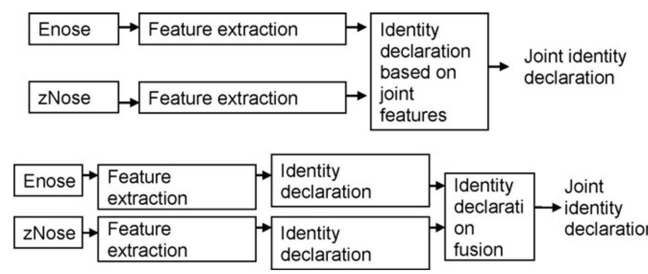

Fig. 2. Feature level (top) and decision level fusion schemes.

2.2. Data fusion schemes

Multisensor fusion provides a collaborative approach to improve classification accuracy by using multiple sensors. Four steps were followed to accomplish multisensor data fusion:

(1) Acquire apple headspace volatile smellprints using the Enose and zNose.
(2) Select and apply the proper multisensor data fusion method. Bayesian classifiers and ANN classification method were applied at feature level and decision level.
(3) Evaluate the multisensor data fusion models by comparing their performance to the previous individual sensor classification models.
(4) The proposed sensor fusion method was accepted, rejected, or refined based on classification error rate.

Two levels of data fusion architecture were investigated in this paper (Fig. 2):

(1) *Feature level fusion*: Features were first extracted by using principal component analysis (PCA) from each source of data (Enose and zNose). These features were concatenated into a single feature vector, which in turn was used as input to artificial neural network for classification.
(2) *Decision level fusion*: Data from each sensor individually was used to perform an identity declaration and the identity declarations provided by the individual sensors were combined using a Bayesian network decision level fusion technique.

The PCA was used for feature extraction. Probabilistic neural networks, backpropagation (BP) networks, and Bayesian networks were used for data fusion and classification. The covariance matrix adaptation evolutionary strategy (CMAES) was used for feature selection from the Enose and zNose and to optimize data fusion models. In the sections that follow, these algorithms are introduced.

2.3. Principal component analysis

Principal component analysis (PCA) is a linear projection of multidimensional data onto different coordinates based on maximum variance and minimum correlation. As a result, less

Table 1
Sampling protocol for the Enose

Period of sampling	Sampling time (days after cutting)	No. of replications	No. of samples	Data set
March 2005	5, 7, 9, 11, 14	24	120	1
June 2005	4, 6, 8, 10	24	96	2
September 2005	5, 7, 9, 11, 13	48	240	3
Total			456	Pooled

significant components can be eliminated, reducing the data representation to only those responsible for the most significant contribution. PCA was used for feature extraction. The data were processed by PCA and only the principal components that explained more than 0.5% of the variance were selected. Based on this rule, the first five principal components were extracted from the Enose data, the first 11 principal components were extracted from the zNose data, and the first six principal components were selected from fused raw data of the Enose and zNose.

2.4. PNN and BP networks

A probabilistic neural network (PNN) was designed for feature-based data fusion models. The PNN consisted of an input layer, radial basis layer, competitive layer and output layer [30]. The number of elements in the input layer was set to the total number of principal components extracted from the Enose (5 PCs) and zNose (11 PCs). The number of neurons in the hidden layer was set to the size of the training data set. Neurons in the output layer were set to two, which represented two classes: healthy and damaged apples. The total of 456 data vectors were divided into a training set (342 vectors) and a testing set (114 vectors).

A three layer back propagation (BP) neural network was developed for decision level sensor fusion. The first five principal components (PCs) from the Enose and the first 11 PCs from the zNose were used for inputs. The number of hidden layer neurons was determined by trial-and-error, and set at 30. The output layer has two neurons to represent healthy and damaged apples. The tan-sigmoid function was used as the hidden layer transfer function and the log-sigmoid was used as the output layer transfer function, which can be expressed in the following forms:

$$\log\,\mathrm{sig}(n) = \frac{1}{1+\mathrm{e}^{-n}} \tag{1}$$

$$\tan\,\mathrm{sig}(n) = \frac{2}{1+\mathrm{e}^{-2n}} - 1 \tag{2}$$

2.5. CMAES

As a state-of-the-art version of the evolutionary strategy, the covariance matrix adaptation evolutionary strategy (CMAES) is a heuristic optimization algorithm which can be used to select the most relevant features from a multivariate space [31]. For the Enose, the 32 sensors were considered decision variables to select; for the zNose, the continuous chromatograph, consisting of 512 wavelength values, was divided into 64 windows and each window with eight wavelength values was treated as one decision variable to select, which greatly reduced the number of decision variables.

The initial population is generated by sampling a normal distribution with a user-specified mean value and standard deviation for each decision variable. Offspring generation, selection and recombination, covariance matrix adaptation, and step size control are four key operators in the process of evolution [31].

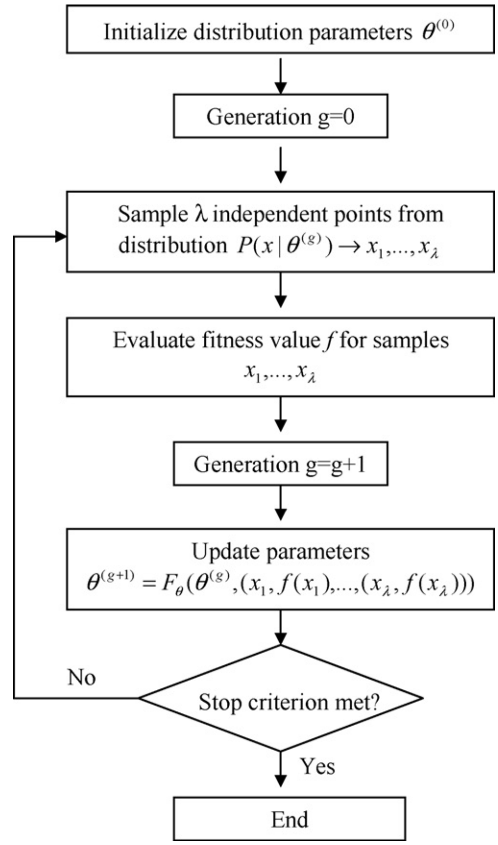

Fig. 3. CMAES algorithm flow chart.

CMAES can be described as a randomized black box search whose computation flowchart is shown in Fig. 3.

The goal is to find decision variables $x \in R^n$, with the minimum cost function values $f(x)$. The cost function value is defined as the classification error rate computed by PNN or BP network, as shown in Eq. (3). The fitness value is the opposite of the cost value, determined by adding a minus sign in front of Eq. (3). F_θ is the joint fitness value of f with current distribution parameters θ at generation g:

$$\text{classification error rate} = \frac{\text{number of misclassifications}}{\text{number of testing set samples}} \tag{3}$$

Proper selection of algorithm parameters is important for search efficiency, global optimization quality, and algorithm reliability. In CMAES, the following parameters were used: λ, μ, w_i, c_{cov}, c_{c}, μ_{cov}, c_σ and d_σ [31]. Among them, population size λ, parent number μ and recombination weight w_i are given in the algorithm [31]. The default values are defined in Eqs. (4)–(6) and other parameters can be derived using these three parameters:

$$\lambda = 4 + [3\ \ln\, n] \tag{4}$$

$$\mu = \frac{\lambda}{2} \tag{5}$$

$$w_i = \frac{\ln(\mu+1) - \ln\, i}{\mu\ \ln(\mu+1) - \sum_{j=1}^{\mu} \ln\, j}, \quad \text{for } i = 1, \ldots, \mu \tag{6}$$

where n is the number of decision variables.

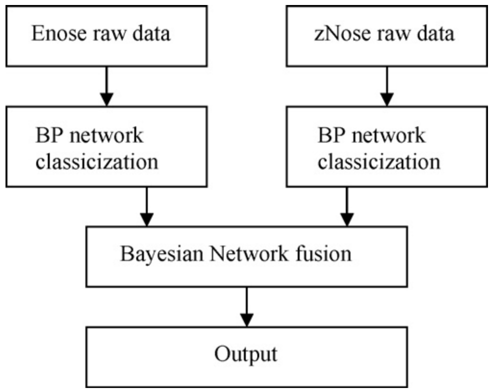

Fig. 4. Bayesian fusion flowchart.

The stop criteria for the Enose sensor selection application is when the maximum standard deviation of the decision variables is smaller than 0.25 or the cost value reaches its global minimum of 0.

2.6. Bayesian network fusion

A simple Bayesian network was constructed to fuse the output from the BP neural network classifiers for cases where the Enose and zNose classifiers were in disagreement. The Bayesian fusion flowchart and Bayesian network structure are shown in Figs. 4 and 5. As a result of the conditional independence relations associated with the structure of the Bayesian network, the joint probability distribution can be factored as

$$P(X) = \prod_{i=1}^{n} P(x_i|pa(x_i)) \tag{7}$$

where X is the set of random variables (RVs) associated with the nodes in the network, x_i the ith RV, and $pa(x_i)$ are the set of RVs (nodes) which are the parents of x_i. For the Bayesian Network this factorization results in

$$\begin{aligned}(\text{Apple, Enose, zNose, EnoseANN, zNoseANN}) \\ = P(\text{Apple})P(\text{Enose}|\text{Apple})P(\text{zNose}|\text{Apple}) \\ \times P(\text{EnoseANN}|\text{Enose})P(\text{zNoseANN}|\text{zNose})\end{aligned} \tag{8}$$

The conditional probabilities $P(\text{EnoseANN}|\text{Enose})$ and $P(\text{zNoseANN}|\text{zNose})$ represent the uncertainty in the BP neural network classification results for the Enose and zNose, respectively. These parameters are often termed the observation or sensor model. The values for these conditional probabilities were obtained from the output neurons from the neural network. These values can be viewed as the strength of the support (or likelihood) that the classifier has determined for each of the decision (output) nodes. For example, if the neural network classifier has determined the following values for the decision nodes for analyses of a given apple with both Enose and zNose:

$$\text{Enose} = [\text{good} = 0.8\ \text{bad} = 0.2] \quad \text{and}$$

$$\text{zNose} = [\text{good} = 0.4\ \text{bad} = 0.6]$$

then the classifier would select “good” for the Enose measurement and “bad” for the zNose measurement. The conditional probabilities $P(\text{EnoseANN}|\text{Enose})$ and $P(\text{zNoseANN}|\text{zNose})$ for this case then would be:

$$P(\text{EnoseANN}|\text{Enose}) = \begin{bmatrix} 0.8 & 0.2 \\ 0.2 & 0.8 \end{bmatrix} \quad \text{and}$$

$$P(\text{zNoseANN}|\text{zNose}) = \begin{bmatrix} 0.4 & 0.6 \\ 0.6 & 0.4 \end{bmatrix}$$

The conditional probabilities $P(\text{Enose}|\text{Apple})$ and $P(\text{zNose}|\text{Apple})$ could be used to incorporate prior independent information regarding the performance of the Enose and zNose instruments given a good or bad apple. In this case, a 2×2 identity matrix for these parameters was used. Finally, the prior probability distribution for the “Apple” RV is set to [0.5 0.5] since the Bayesian network was only used for cases where the Enose and zNose classifications were in conflict.

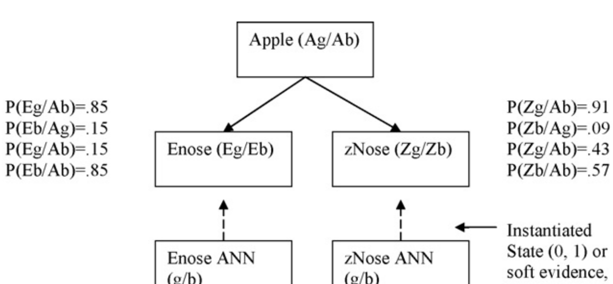

Fig. 5. Bayesian network structure.

3. Computational experiment

3.1. CMAES coding methods comparison

If each Enose sensor (32 total) and zNose wavelength window (64 total) is considered as one variable, there are 96 variables to consider. The chromosome (which consists of decision variables) will be too long if binary coding methods are used, which reduces the computational efficiency. To reduce chromosome length (i.e. number of decision variables) and at the same time fully exploit the advantage of CMAES for solving continuous number problems, a real number coding scheme was developed. Two different length real number coding schemes for the CMAES were developed and compared.

3.1.1. 48-Variable scheme

Each variable was evenly divided into four segments, and each segment represented one out of four possibilities of two sensors selected, as defined in Eq. (9). For instance, if x falls into the range of [0.25, 0.5), it represents the state of [1,0] that the first sensor was selected and the second was not selected. By doing this, a total of 96 decision variables can be represented by 48 real number variables. This reduced the variable number by

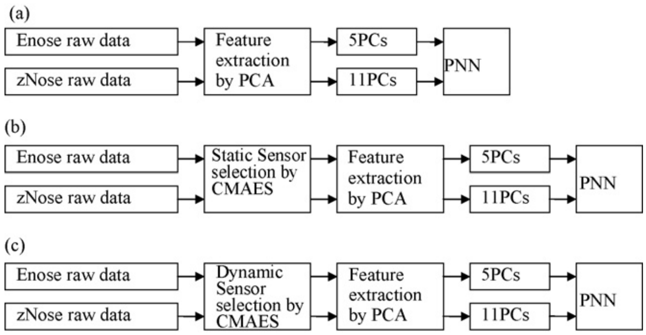

Fig. 6. Three ANN fusion schemes: (a) non-selective fusion; (b) static selective fusion; (c) selective fusion.

50% compared to binary coding.

$$x \in \begin{cases} [0, 0.25) \Rightarrow [0, 0] \\ [0.25, 0.50) \Rightarrow [1, 0] \\ [0.50, 0.75) \Rightarrow [0, 1] \\ [0.75, 1.00] \Rightarrow [1, 1] \end{cases} \tag{9}$$

3.1.2. 24-Variable coding scheme

Similarly, a 24-variable coding scheme can be carried out by using only one real number variable to represent 16 possible selections for four sensors (Eq. (10)).

$$x \in \begin{cases} [0.0000, 0.0625) \Rightarrow [0, 0, 0, 0] \\ [0.0625, 0.1250) \Rightarrow [0, 0, 0, 1] \\ [0.0125, 0.1875) \Rightarrow [0, 0, 1, 0] \\ [0.1875, 0.2500) \Rightarrow [0, 0, 1, 1] \\ [0.2500, 0.3125) \Rightarrow [0, 1, 0, 0] \\ [0.3125, 0.3750) \Rightarrow [0, 1, 0, 1] \\ [0.3750, 0.4375) \Rightarrow [0, 1, 1, 0] \\ [04375, 0.5000) \Rightarrow [0, 1, 1, 1] \\ [0.5000, 0.5625) \Rightarrow [1, 0, 0, 0] \\ [0.5625, 0.6250) \Rightarrow [1, 0, 0, 1] \\ [0.0625, 0.6875) \Rightarrow [1, 0, 1, 0] \\ [0.6875, 0.7500) \Rightarrow [1, 0, 1, 1] \\ [0.7500, 0.8125) \Rightarrow [1, 1, 0, 0] \\ [0.8125, 0.8750) \Rightarrow [1, 1, 0, 1] \\ [0.8750, 0.9375) \Rightarrow [1, 1, 1, 0] \\ [0.9375, 1.0000) \Rightarrow [1, 1, 1, 1] \end{cases} \tag{10}$$

By doing this, the number of decision variables can be further reduced from 48 to 24, which can reduce population size and computation time.

3.2. Three feature level fusion schemes comparison

At the feature level, three schemes were proposed and tested, as shown in Fig. 6.

(1) Non-selective fusion scheme: this scheme uses all raw data without data dimension reduction.
(2) Static selective fusion scheme: this scheme is different from the first scheme in that it uses only partial raw data which were previously selected by CMAES. The 7 sensors and 32 wavelength windows were selected for the Enose and zNose individually by the CMAES.
(3) Dynamic selective fusion scheme: in contrast to the static selective fusion, this scheme combines all decision variables (32 from the Enose and 64 from the zNose) and uses the CMAES to dynamically select sensors (variables) from the Enose and zNose simultaneously.

4. Results

4.1. Two coding methods comparison

Two real number coding methods (48-variable and 24-variable) were executed by the CMAES and their search performances were compared. Fig. 7 shows a typical search history for a 48-variable coding method: the CMAES with the 48-variable real number coding can effectively reduce the classification error rate from 0.16 at the beginning to 0 at the end of the search.

Since the evolutionary strategy is a heuristic search method and each run may return a different search result, two coding methods were executed 30 times each with 30 random seeds. Different random seeds generate different populations (or initial sensor selection), and they follow different evaluation paths, so their final search results may be different. Three performance parameters were compared in Table 2: the best fit value or minimum cost value which is a measure of search quality, the number of function evaluations (NFE) which is a measure of search efficiency, and the number of sensors selected from the Enose and zNose, which is a measure of dimensionality reduction. It is observed that both coding methods can reduce the classification error rate to 0 which appeared three times in both cases. Their 30-time run average performances are comparable, 1.7% versus 1.8% error rate. However, the 48-variable real number coded CMAES was more efficient than its coun-

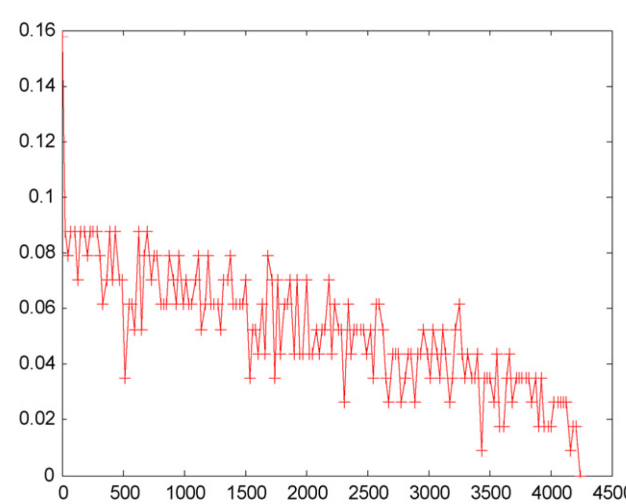

Fig. 7. A typical 48-variable search history by the CMAES.

Table 2
48-Variable and 24-variable coded CMAES for sensor fusion searching (over 30 random runs)

No.	48-Variable coding method				24-Variable coding method			
	Minimum cost	NFE	Enose sensors	zNose sensors	Minimum cost	NFE	Enose sensors	zNose sensors
1	2	3152	17	31	1	3252	20	30
2	1	3452	11	29	2	5202	14	29
3	2	3602	18	26	2	4318	24	26
4	2	3622	12	32	0	4292	18	29
5	1	4082	17	35	2	4240	24	35
6	1	4172	14	33	3	4838	20	29
7	0	4172	22	29	3	4682	20	30
8	2	3182	12	32	1	4266	20	34
9	2	3962	9	38	3	4006	17	26
10	2	3662	19	36	0	2576	23	31
11	3	3272	21	27	2	3434	20	32
12	2	3962	19	37	2	5098	13	35
13	1	3902	8	30	2	5046	15	36
14	2	5462	17	26	2	4500	24	36
15	2	3782	23	27	1	3512	10	30
16	2	4682	13	39	3	4552	19	33
17	2	4532	24	39	3	4578	17	24
18	1	4232	17	29	3	2862	17	33
19	1	3632	14	29	1	4734	18	31
20	0	4232	18	31	1	3928	20	30
21	2	3962	16	29	2	5202	19	34
22	4	3392	13	29	1	4968	18	34
23	1	5012	11	35	2	4759	18	30
24	1	4472	8	32	2	4474	11	33
25	2	3092	17	27	3	6268	23	28
26	2	3992	16	27	2	5826	19	32
27	2	3962	13	31	2	5618	21	30
28	0	2972	12	26	0	4240	25	32
29	2	3572	17	35	1	6216	15	33
30	3	3392	19	37	2	3616	22	29
Average	1.7	3886	16	31	1.8	4503	19	31

terpart, using only 3386 function evaluations, 25% less than that of 24-variable real number coded CMAES. Considering the dimensionality reduction, both schemes reduced zNose chromatograph windows from 64 to 31 (52% reduction), while the 48-variable scheme reduced more Enose data dimensionality (50%) than did the 24-variable scheme (41%). Thus, the 48-variable scheme was recommended for feature selection in this data fusion application. Fig. 8 is an illustration of selected wavelength windows from the zNose and sensors from the Enose. The red dashed line represents removed wavelength windows, in which the blue solid line (selected wavelengths) was set to 0.

For the best scenario, when the classification error rate was 0 and the least sensors were selected from both the Enose and zNose, the following sensors/wavelength windows were selected:

- Selected sensors from the Enose (22): 3 5 6 8 10 11 12 13 14 15 16 17 18 19 20 21 24 26 28 30 31 32
- Selected wavelength windows from the zNose (29): 1 2 5 6 7 8 11 12 13 18 19 20 22 23 24 28 34 45 46 47 50 54 57 59 60 61 62 63 64

4.2. Feature level data fusion comparison

Based on the methods presented above, three feature level data fusion schemes were executed and compared (Table 3). In the non-selective scheme, all 32 sensors from the Enose and

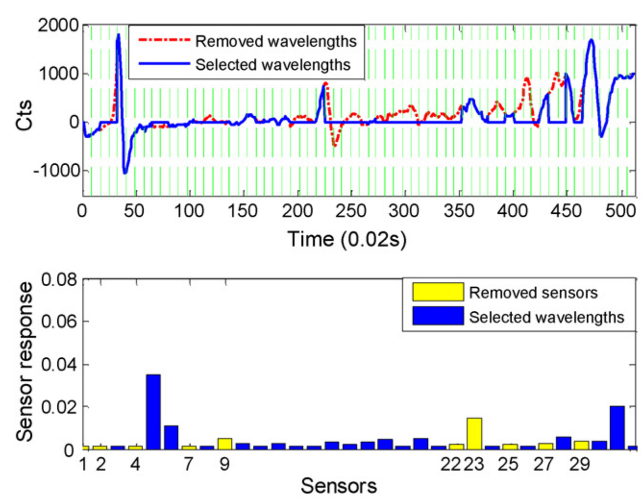

Fig. 8. Selected sensors from the zNose (top) and Enose (bottom).

Table 3
Classification error rate comparison between sensor fusion schemes and individual sensors

Schemes	Individual sensor		Sensor fusion
	Enose	zNose	Enose + zNose
Non-selective	15%	23%	32.5%
Dynamic selective (for individual sensors)/static selective (for fusion)	4.2%	2.6%	6.1%
Dynamic selective (for sensor fusion)	N/A	N/A	1.5%

64 zNose spectral windows were used separately and jointly for development of classification models. In this case, the sensor fusion model which combined all sensors yielded a 32.5% error rate which was not better than individual sensor models (15% and 23% error for the Enose and zNose, respectively). In the static selective fusion scheme, the Enose and zNose sensors which were selected separately were jointly used in the sensor fusion model. The classification error rate was reduced from 32.5% to 6.1%. In the third scenario, all 32 sensors from the Enose and 64 windows from the zNose were jointly coded in one chromosome and dynamically selected using the CMAES, and the selected sensors were fed into the PNN-based sensor fusion model. The results were encouraging: the dynamic selective sensor fusion model achieved an average 1.5% error rate in 30 independent runs, which outperformed the individual sensor classification models.

4.3. Decision level Bayesian network fusion

At the decision level, a Bayesian network, based on Bayesian decision rules, was developed. The Bayesian network utilizes the classification results obtained independently from the Enose and zNose neural network classifiers, to make its fused decision. The Enose and zNose classifiers may have classification decisions that agree or conflict. In the situation where both classifiers make the same wrong decisions, there is no way to use Bayesian fusion to improve the classification results. In the situation of decision conflict between two classifiers, there must be one correct and one wrong, and the Bayesian network fusion is designed to reduce error in such cases using the likelihood outputs from the neural network (see Section 2.6).

4.3.1. BP soft/hard evidence Bayesian fusion

Both the Enose and zNose BP neural network classifiers produced real value outputs, which indicate the likelihood of the sample belonging to certain classes. By using this information, the Bayesian fusion was expected to reduce the overall error rate.

The simulation results in Table 4 show the Bayesian network performance results yielding an overall error rate of 11%, which was better than the error rates for the individual sensors (13% and 20% error rate for the Enose and zNose, respectively).

5. Discussion

Based on the feature selection results using the CMAES, both the Enose and zNose have redundant sensors. However, the zNose raw data have more noise and irrelevant information than that of the Enose. The zNose data are more compressible, e.g., using all 512 wavelengths gave a classification error rate of 23%, but after reducing its data dimensionality by 50%, the error rate was reduced to 2.6%. For the Enose, the number of sensors was reduced 40–50% while the classification error rate was reduced from 15% to 4.2%. This indicates that the zNose has more irrelevant sensors, which adds noise and worsens the classification result, while the Enose has more sensors that are highly correlated with each other and redundant.

By comparing three feature-based fusion schemes, it was found that simply adding the Enose and zNose raw data together in non-selective feature fusion worsened the classification results: the 32.5% error rate from the fused data is higher than from the Enose (15%) and the zNose (23%) individually. The static selective fusion scheme did not make sensor fusion superior to using the Enose or zNose alone. The dynamic selective fusion which jointly selected useful features from the Enose and zNose greatly improved the system performance with a 0 classification error rate. This result is better than using either of these two instruments alone. Although static selective fusion used the selected sensors, these sensors were selected from the Enose and zNose separately. They may work well individually, but not provide complementary information when they are put together. In contrast, the dynamic selective sensor fusion selected only the sensors providing complementary information and consequently resulted in a better classification performance than using the Enose or zNose individually.

At the decision level, a Bayesian network fusion was used to process data from BP neural network classifier. The Bayesian network fusion model achieved better results than each individual classifier alone by utilizing the "soft evidence" (likelihood) output from the neural network. This is because the likelihood from the NN provides information on the "strength" of its belief that a particular sample is associated with a certain class. Generally, when more information is used, better results are achieved.

Table 4
Three Bayesian fusion schemes performance comparison

	Enose	zNose	Bayesian network fusion
Error rate	13%	20%	11%
Error 1[a]	25		7
Error 2[b]	6		6

[a] Error 1 is defined as the number of errors caused by the Enose and zNose decisions conflict.

[b] Error 2 is defined as the number of errors caused by the Enose and zNose when both made the wrong decision.

Comparing the feature level and decision level data fusion models, the dynamic selective feature level data fusion achieved better performance (average 1.5% error rate) than the decision level data fusion (11% error rate). The decision level fusion's performance depends on the performances of the two instruments. By using soft evidence from BP classifiers, Bayesian network fusion can improve the individual sensors' performance by 2%. These results supported the claim [21] that generally better accuracy is obtained by fusing information closer to the source. With higher level fusion more information is lost, although at lower level fusion, more noise would be added to the model. Using optimization methods such as evolutionary strategy to select the most relevant features and remove redundant sensors and noise is a good choice for feature level fusion.

6. Conclusions

In this paper, feature level and decision level multisensor data fusion models, used to combine the Enose and zNose for apple defect detection, were developed and compared. In the feature level fusion, the covariance matrix adaptation evolutionary strategy, an optimization algorithm, was incorporated into the fusion process and used for feature selection. Two real number coding methods were constructed and results showed that 48-variable coding performed slightly better than 24-variable coding when search quality, search efficiency, and dimensionality reduction were considered. Based on whether or not the feature selection was carried out, three feature-based fusion schemes were developed and compared. Among them, the dynamic selective fusion outperformed the other two schemes, with a best case of 0% and average performance of 1.8% classification error rate in total 30 independent runs. In the decision level fusion, Bayesian network fusion using soft evidence from the BP neural network improved individual sensor's performance by 2%, while using hard evidence and prior performance gave results only as good as one of the two instruments. The dynamic selective fusion model provided the best performance, which supports the claim that in multisensor data fusion, generally, a better result is obtained at lower level data fusion because less original information is lost.

This research developed multisensor data fusion models to integrate two volatile detection instruments (the Enose and zNose) for apple defect detection. By improving the detection accuracy, this non-destructive measurement system could detect spoiled or diseased apples with more reliability, which not only reduces economic losses from grocery stores, but safeguards our food supply chain and protects consumers' health as well.

Acknowledgement

The authors would like to thank Dr. David Hall for his insights and useful discussions.

References

[1] USDA-NASS, 2004–2005 Statistical highlight of US agriculture: Crops; 2006 [cited 2006 June 23]. Available from: http://www.usda.gov/nass/pubs/stathigh//2005/cropindex.htm.

[2] USDA-FAS, World apple situation [cited 2006 June 23, 2006]; 2005. Available from: http://www.fas.usda.gov/htp/horticulture/Apples.

[3] A. Vikram, B. Prithiviraj, A.C. Kushalappa, Use of volatile metabolite profiles to discriminate fungal diseases of Cortland and Empire apples, J. Plant Pathol. 86 (2004) 215–225.

[4] NE179, Technology and principles for assessing and retaining postharvest quality of fruits and vegetables, 2001. Available at: http://www.nimss.umd.edu/homepages/home.cfm?trackID=23.

[5] J.E. Simon, A. Hetzroni, B. Bordelon, G.E. Miles, D.J. Charles, Electronic sensing of aromatic volatiles for quality sorting of blueberries, J. Food Sci. 61 (1996) 967–969.

[6] K. Persaud, G.H. Dodd, Analysis of discrimination mechanisms in the mammalian olfactory system using a model nose, Nature 299 (1982) 352–355.

[7] E. Schaller, J.O. Bosset, F. Escher, Electronic Noses and their application to food, Lebensmittel-Wissenschaft und-Technologie 31 (1998) 305.

[8] E.R. Thaler, D.W. Kennedy, C.W. Hanson, Medical applications of electronic nose technology: review of current status, Am. J. Rhinol. 15 (2001) 291–295.

[9] S.S. Schiffman, B.G. Kermani, H.T. Nagle, Analysis of medication off-odors using an electronic nose, Chem. Senses 22 (1997) 119.

[10] E. Llobet, E.L. Hines, J.W. Gardner, S. Franco, Non-destructive banana ripeness determination using a neural network-based electronic nose, Meas. Sci. Technol. 10 (1999) 538–548.

[11] S. Oshita, K. Shima, T. Haruta, Y. Seo, Y. Kawagoe, S. Nakayama, H. Takahara, Discrimination of odors emanating from 'La France' pear by semi-conducting polymer sensors, Comp. Electron. Agric. 26 (2000) 209.

[12] J. Brezmes, E. Llobet, X. Vilanova, J. Orts, G. Saiz, X. Correig, Correlation between electronic nose signals and fruit quality indicators on shelf-life measurements with pinklady apples, Sens. Actuators B: Chem. 80 (2001) 41.

[13] S. Balasubramanian, S. Panigrahi, C.M. Logue, M. Marchello, C. Doetkott, H. Gu, J. Sherwood, L. Nolan, Spoilage identification of beef using an electronic nose system, Trans. ASAE 47 (2004) 1625–1633.

[14] G.S. Osborn, R.E. Lacey, C. Aboukinane, A method to detect peanut off-flavors using an electronic nose, Trans. ASAE 44 (2001) 929–938.

[15] T. Eklov, G. Johansson, F. Winquist, I. Lundstrom, Monitoring sausage fermentation using an electronic nose, J. Sci. Food Agric. 76 (1998) 525–532.

[16] A. Jonsson, F. Winquist, J. Schnurer, H. Sundgren, I. Lundstrom, Electronic nose for microbial quality classification of grains, Int. J. Food Microbiol. 35 (1997) 187.

[17] M. Benady, J.E. Simon, D.J. Charles, G.E. Miles, Fruit ripeness determination by electronic sensing for aromatic volatiles, Trans. ASAE 38 (1995) 251–257.

[18] J.W. Gardner, H.V. Shurmer, T.T. Tan, Application of an electronic nose to the discrimination of coffees, Sens. Actuators B: Chem. 6 (1992) 71–75.

[19] D.L. Hall, An introduction to multisensor data fusion, in: Proceedings of the IEEE, vol. 85, 1997, pp. 6–23.

[20] D.L. Hall, J. Llinas, Handbook of Multisensor Data Fusion, CRC Press, Boca Raton, FL, 2001.

[21] D.L. Hall, S.A.H. McMullen, Mathematical Techniques in Multi-sensor Data Fusion, 2nd ed., Artech House, Boston, 2004.

[22] V. Steinmetz, M. Crochon, V. Bellon-Maurel, J.L. Garcia Fernandez, P. Barreiro Elorza, L. Verstreken, Sensors for fruit firmness assessment: comparison and fusion, J. Agric. Eng. Res. 64 (1996) 15–28.

[23] S. Roussel, V. Bellon-Maurel, J.-M. Roger, P. Grenier, Fusion of aroma, FT-IR and UV sensor data based on the Bayesian inference. Application to the discrimination of white grape varieties, Chemometrics Intelligent Lab. Syst. 65 (2003) 209.

[24] S. Roussel, V. Bellon-Maurel, J.-M. Roger, P. Grenier, Authenticating white grape must variety with classification models based on aroma sensors, FT-IR and UV spectrometry, J. Food Eng. 60 (2003) 407.

[25] V. Steinmetz, J.M. Roger, E. Molto, J. Blasco, On-line fusion of colour camera and spectrophotometer for sugar content prediction of apples, J. Agric. Eng. Res. 73 (1999) 207.

[26] N. Ozer, B.A. Engle, J.E. Simon, Fusion classification techniques for fruit quality, Trans. ASAE 38 (1995) 1927–1934.

[27] C. Li, P. Heinemann, J. Irudayaraj, Detection of apple defects using an electronic nose and zNose, Trans. ASABE, accepted.
[28] J. Lammertyn, E. Veraverbeke, J. Irudayaraj, zNose(TM) technology for the classification of honey based on rapid aroma profiling, Sens. Actuators B: Chem. 98 (2004) 54.
[29] Cyrano Science Inc., Cyranose 320 Users Manual, 2000.
[30] H. Demuth, M. Beale, Neural Network Toolbox User's Guide: Version 4, The Mathworks, 2001.
[31] N. Hansen, The CMA Evolution Strategy: A Tutorial, 2005. Available at: http://www.inf.ethz.ch/personal/hansenn/index.html.

Biographies

Changying Li received his PhD degree from the Department of Agricultural and Biological Engineering at the Pennsylvania State University, University Park in 2006. He is currently a postdoctoral fellow at the University of Illinois at Urbana-Champaign. His research interests are in systems modeling, sensors and instrumentation.

Paul Heinemann, PhD, is a Professor in Department of Agricultural and Biological Engineering at the Pennsylvania State University, University Park. His research interests are in systems modeling, mushroom production, and sensor evaluation.

Richard Sherry is a Senior Research Associate in the School of Information Sciences and Technology at the Pennsylvania State University. He holds a PhD in Information Sciences and Technology from the Pennsylvania State University, a MS in Nuclear Engineering from the University of Michigan and a BS in Nuclear Engineering from the Pennsylvania State University. His research interests include knowledge representation, machine learning, inference, information fusion and decision-making in real world complex domains that are characterized by large amounts of uncertainty. His research has focused on the use of probabilistic graphical models such as Bayesian networks, influence diagrams, and Markov decision processes.